Journal of Coastal Research	SI	116	61-65	Charlotte, North Carolina	2023

Impacts of Marine Construction on Tidal and Residual Characteristics: An Example from the Incheon Bridge

Myung Hwan Kim†, Seung-Buhm Woo†, Hye Min Lee†, Ki-Hwan Kim†, Jin-Il Song†, and Jong Wook Kim†*

†Department of Oceanography
Inha University
Incheon, Republic of Korea

www.cerf-jcr.org

www.JCRonline.org

ABSTRACT

Kim, M.H.; Woo, S.-B.; Lee, H.M.; Kim, K.-H.; Song, J.-I., and Kim, J.W., 2023. Impacts of marine construction on tidal and residual characteristics: An example from the Incheon Bridge. *In:* Lee, J.L.; Lee, H.; Min, B.I.; Chang, J.-I.; Cho, G.T.; Yoon, J.-S., and Lee, J. (eds.), *Multidisciplinary Approaches to Coastal and Marine Management*. *Journal of Coastal Research*, Special Issue No. 116, pp. 61-65. Charlotte (North Carolina), ISSN 0749-0208.

This study examined the effects on tidal and residual characteristics resulting from the reduction in channel width due to the construction of the Incheon Bridge (IB). Using the three-dimensional numerical model two scenarios were simulated without and with the construction of the IB. Installed piers from the IB construction changed the characteristics of flood and ebb tides, especially near the bridge. As a result, the ebb-dominance on the north side of the navigation channel near the bridge is weakened, and the ebb-dominance on the south side is strengthened. Due to these changes in tidal asymmetry, the residual flow velocity of all vertical layers on the north side of the navigation channel is increased to the ebb direction, strengthening the vertical two-layer circulation. On the other hand, on the south side of the channel, the residual flow velocity of all vertical layers is increased in flood direction, unifying the residual direction of all vertical water columns to the ebb direction. Therefore, the influence of marine constructions such as bridges can play an important role in numerical model studies on tidal and residual characteristics of coastal regions.

ADDITIONAL INDEX WORDS: *Incheon Bridge, tidal asymmetry, residual current.*

INTRODUCTION

Residual currents play an important role in net mass transport in the macrotidal estuary (Yanagi *et al.*, 2003). In macrotidal estuaries, it has been known that the residual flow patterns were affected by the increase in nonlinearity process due to overtide (Wang, Jeuken, and De Vriend, 1999) and the vertical and horizontal density structures caused by the increase in freshwater inflow. In addition, since the estuary is continuously affected by artificial influences such as tidal power plants, dams, estuary banks, and submerged structures for human activities, it also leads to changes in residual flow patterns as a result. For instance, in the Rance estuary, the pattern of residual flow changed due to the discharge of the La Rance tidal power plant (Kirby and Retière, 2009). Yamini *et al.* (2021) suggested that the vertical residual structure caused by dam discharge can be very considerable in reservoirs depending on the type of sluice structure of the dam. For Jiaozhou Bay, China, Li *et al*. (2014) mentioned an important environmental change as the residual flow velocity decreased at the entrance of the bay after the construction of the bridge and the ability of water exchange also decreased.

Gyeonggi Bay is located on the west coast of South Korea and is a macrotidal estuary with a tidal range of 8 m or more. Over the past 50 years, the marine infrastructures such as the reclamation of Yeongjongdo, dredging for maintaining the port, and topographical changes due to the construction of the Incheon Bridge (IB) have been installed, resulting in problems such as port siltation, marine debris, and beach erosion. Among them, IB, completed in 2009, is the longest bridge in South Korea with a length of about 21.38 km connecting Yeongjongdo and Songdo. With the construction of the IB, 192 piers were installed in the surrounding sea regions, and the cross-sectional area of the navigation channel was reduced. It has been reported that the increase in the sedimentation and the flow environment are strongly affected by the construction of this bridge (Yeo *et al*., 2006; Yeo *et al*., 2008). But, there are few research results that quantitatively suggest how the residual flow pattern is changed by the construction.

Lee, Kim, and Woo (2023) studied the salt transport mechanism in Gyeonggi Bay using a Finite Volume Community Ocean Model (FVCOM). However, in the aforementioned study, the grid corresponding to the IB was not applied, so it was not possible to directly evaluate the change of residual flow. Therefore, in this study, a simulation was performed to evaluate the effect of the IB construction on the residual flow pattern by modifying the resolution of the FVCOM grid used by Lee, Kim, and Woo (2023).

The purposes of this study are (1) to examine changes in tidal flow patterns, (2) quantitative comparison of horizontal and vertical structures of residual currents, and (3) the correlation between the residual flow structure and salinity due to the construction of the IB.

DOI: 10.2112/JCR-SI116-013.1 received 6 March 2023; accepted in revision 21 April 2023.
*Corresponding author: kaonesis@gmail.com

METHODS

The FVCOM developed by the University of Massachusetts Dartmouth and Woods Hole Oceanographic Institution was used to analyze the tidal and residual characteristics changes induced by the construction of IB in Gyeonggi Bay. FVCOM uses 3-D primitive equations such as momentum, continuity, temperature, salinity, and density equations. In addition, FVCOM can efficiently reproduce the complex coastal boundary by using triangular grids. The detailed FVCOM features for the discrete equations and various boundary conditions are described in the FVCOM manual (Chen *et al*., 2013).

Model Setup and Verification

The length of the model domain is about 145 km in the north-south direction and 150 km in the east-west direction. The water depth of the grid was constructed by referring to the bathymetry data of the datum level provided by the Korea Hydrographic and Oceanography Agency (Figure 1a). Five tidal constituents (M_2, S_2, K_1, O_1, and N_2) obtained from the TPXO8-atlas model results were used as the tidal forcing at the seaward open boundary. The observed February salinity data provided by the National Institute of Fisheries Science was interpolated into the salinity boundary condition by averaging in month.

Daily river discharge data collected from Water Resource Management Information System were inputted into the lateral boundary to consider Han River and Imjin River discharge. The Yeseong River has limited freshwater discharge data. Based on the results of Park *et al*. (2002), 15% of the Han River discharge was used as the river discharge condition for the Yeseong River. The initial salinity field was obtained by the model salinity result on January 20, 2020, after a one-year simulation from January 19, 2019, to January 20, 2020.

The scenario without IB construction (Case 1) and a scenario with IB construction (Case 2) were designed to investigate the hydraulic environment changes caused by IB construction (Figures 1b–c). In Case 1, the number of nodes and cells are 60,882 and 115,443, respectively. The grid resolution varied from 70 m to 4,500 m. Minimum of the grid resolution around the IB is about 200 m (Figure 1c). In Case 2, the grid resolution around the IB varied from 20 m to 200 m. The number of nodes and cells in Case 2 increased to 17,299 and 34,164 compared to Case 1, respectively.

The duration of the simulation is from January 20 to March 20, 2020. The velocity and salinity data at M1 were collected from February 4 to March 17, 2020. The model results for tide level, along-channel velocity, and salinity for Case 1 were compared with the observation data in ST1–ST8 and M1. To assess the quantitative model performance, the predicted skill (*Skill*) presented by Willmott (1982) was calculated (Table 1).

Table 1. *Skill assessment for the tide level, along-channel velocity, and salinity.*

Variables	Observations	*Skill*
Tide Level (m)	ST1–ST8	0.99
Along–Channel Velocity (m/s)	M1	0.98/0.99
Salinity (psu)	M1	0.90/0.90

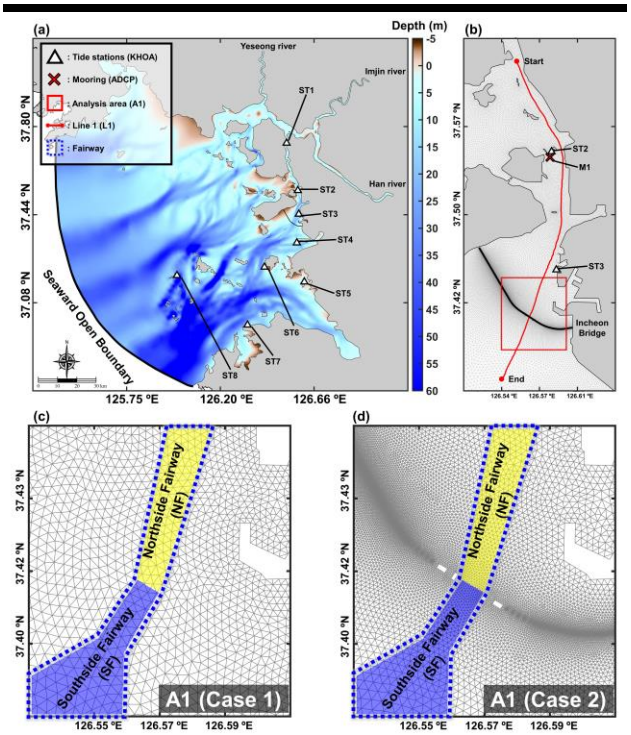

Figure 1. The model domain for the Gyeonggi Bay and comparisons of model grid resolution between without Incheon Bridge (IB) construction (Case1) and with IB construction (Case2). Bathymetry of the model area (a), showing eight tide stations (white triangles, ST1-ST8). An enlarged map showing the vicinity of IB (b). In (b), the red X symbol indicates the mooring, and the red solid line and red square box denote the analysis transect line and region. Model grid resolution for Case 1 (c) and Case 2 (d). The blue and yellow area in (c) and (d) indicates the southside (SF) and northside (NF) of the fairway, respectively.

The model results reproduce the observed tide level variations. The eight tide levels data were compared with tide levels in model results, and *Skill* values at all stations were 0.99. Regarding the observed velocity patterns, the velocity patterns of the model also showed a good evaluation. At M1, the observed and modeled velocity data were converted into the along-channel velocity using Principal Component Analysis (PCA). As a result of comparing the time series of the along-channel velocity between the observed data and the model results, a maximum *Skill* of 0.99 was calculated. Comparisons between the model salinity result and observed salinity data collected by the CTD at M1 resulted in *Skill* values of 0.90 for both surface and bottom layer. The comparison results between observed data and model results indicate that the model reproduces the observed tidal elevation, currents, and salinity well.

RESULTS

The tidal current patterns over a tidal cycle between Case 1 and Case 2 were analyzed. While the boundary conditions and initial conditions of the model are the same for both cases, there is a difference in the increase in grid resolution only according to the 180 piers of the IB. Through this case study, the quantitative tidal strength and direction between Case 1 and Case 2 and the residual flow pattern were presented.

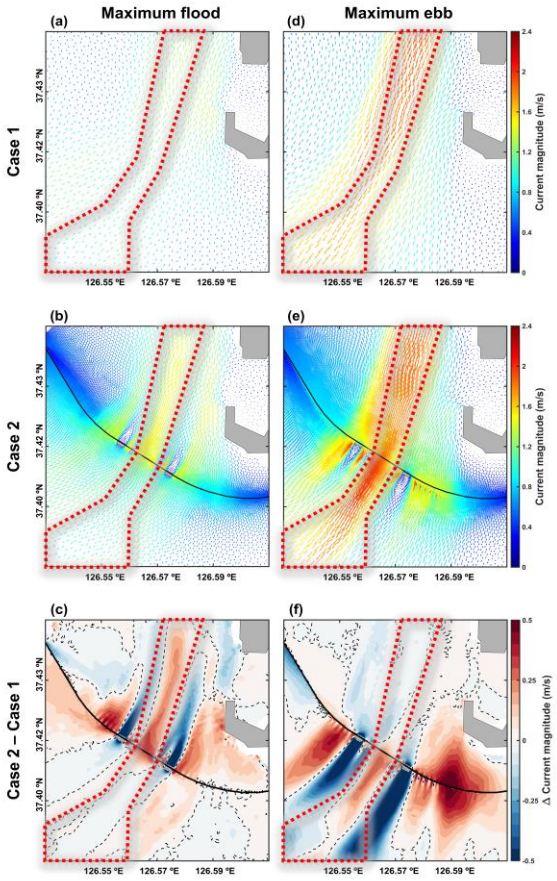

Figure 2. Influence of the IB construction on the near-surface tidal current magnitude in spring tide. (a and d) Maximum flood current magnitude in Case 1 and Case 2. (b and e) Maximum ebb current magnitude in Case 1 and Case 2. The difference at maximum flood tide (c), and maximum ebb tide (f). Thin black dashed line indicates the difference in tidal current magnitude is zero and red dashed line indicates the fairway. Black solid line indicates IB.

Flood and Ebb Currents Variations

The narrow width of at least 50 m between the IB piers increased the magnitude of the tidal current. The differences in tidal current magnitude between the two scenarios (Case 1 and Case 2) at periods of the maximum flood and the maximum ebb are shown in Figure 2. In both cases, the velocity magnitude in the maximum ebb current was greater than that in maximum flood current. And in Case 1 (Figures 2a and d), strong velocities were linearly distributed around the navigation channel (thick black dashed line in Figure 2), but in Case 2 (Figures 2b and e), the velocities were insignificant behind the pier because they were blocked by the structure. On the other hand, relatively strong flow velocities were distributed in the navigation channel between the piers. In addition, the velocity at the center of the main channel in Case 2 was stronger than in Case 1.

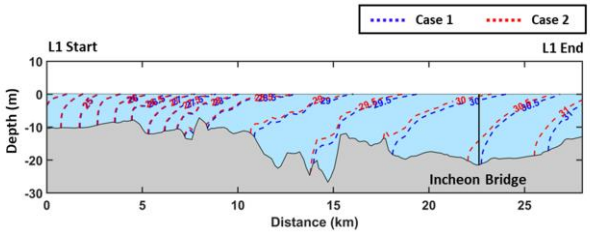

Figure 3. Comparison of horizontal and vertical salinity distribution between Case 1 and Case 2 in analysis line (L1 in Figure 1b). Black solid line indicates the location of IB. Blue- and red- dashed line indicate salinity results in Case 1 and Case 2, respectively.

In the difference between Case 1 and Case 2, the velocity magnitude of the Northside Fairway (NF) increased by 0.33 m/s in the maximum flood current, whereas the velocity magnitude of the Southside Fairway (SF) remained almost unchanged (Figure 2c). In Figure 2f, increase in velocity magnitude occurs on the southern part of IB, and increase in velocity magnitude was greater in the regions passing through the pier than in SF. During this period, the increment in velocity magnitude in SF was about 0.29 m/s, whereas that is about 0.51 m/s around the pier.

Salinity Variations

The monthly time-averaged salinity distribution of the analysis transect line (L1, solid red line in Figure 1b) is presented in Figure 3 to examine the effect of IB construction on the spatial salinity distribution. There was little change in the horizontal and vertical structure of salinity in the northern region (approximately 0 to 10 km distance) of L1 between Case 1 and Case 2. On the other hand, from 10 km of L1 distance to the end of L1, horizontal salinity diffusion in Case 2 occurred less than that in Case 1.

The vertical salinity difference was greater in Case 2 than in Case 1. Overall, the difference in salinity distribution increased as it approached IB. Therefore, due to the IB construction, the vertical gradient of salinity near the IB piers increased and the salinity stratification was strengthened. These distinct salinity structures and stratification changes near IB greatly contribute to the residual flow pattern and tidal asymmetry induced by the density gradient.

Residual Velocity

To analyze the residual flow changes induced by IB construction, a 48-hr low-pass filter was used for the velocity results of the model (Figure 4). The direction of surface residual current in the SF and NF was the ebb direction in both cases (Figures 4a and b). After the IB construction, the residual current velocity decreased in the NF and increased in the SF. The residual velocity magnitude of NF was reduced by a maximum of 0.06 m/s and increased by a maximum of 0.05 m/s in the case of SF. Interestingly, the residual velocity change was higher at the piers

on both sides of the navigation channel. In particular, the magnitude of the residual velocity increased in the northern part of the IB, while it decreased in the southern part (Figure 4c).

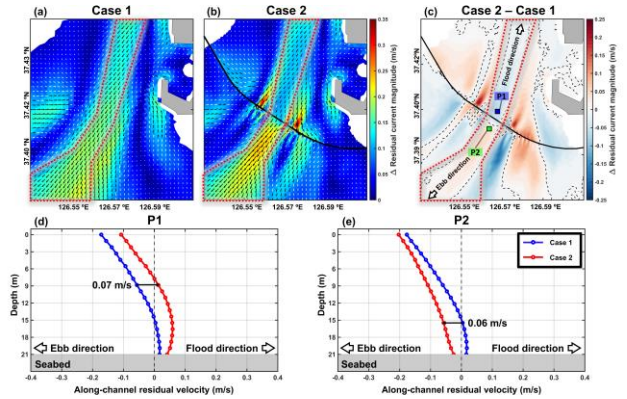

Figure 4. Difference of near-surface tidal current magnitude between Case 1 and Case 2 (Case 2 – Case 1). The difference at maximum flood tide (a), and maximum ebb tide (b). Black dashed line indicates the difference in tidal current magnitude is zero. (a and b) Black triangle indicates a sandbank, and black solid line indicates IB.

To compare the vertical profile of residual current in Case 1 and Case 2, points P1 and P2 were selected (blue and green squares in Figure 4c). In the case of P1, the along-channel residual velocity increases in the flood direction, strengthening the vertical two-layer flow structure. Conversely, the along-channel residual velocity of P2 increased in the ebb direction, so the residual flow in all vertical water column was unified in the ebb direction.

DISCUSSION

Due to the construction of the IB, not only the residual flow pattern of the navigation channel, but also the residual flow patterns on both sides of the channel significantly changed. These changes can be attributed to the asymmetry between flood and ebb currents over a tidal cycle. It is known that tidal asymmetry is most affected by topographical conditions related to bottom friction and affects changes in the vertical structure of residual flow.

To analyze the spatial changes in tidal deformation, the tidal asymmetry parameter (γ^0) calculated as follows using the equation given by Nidzieko and Ralston (2012):

$$\gamma^0 = \frac{\mu_3}{\mu_2^{3/2}} \quad (1)$$

$$\mu_m = \frac{1}{N-1}\sum_{i=1}^{N}(X_i)^m \quad (2)$$

where, μ_m is the m-th moment about zero, N is the data length, and X_i is the i-th along-channel velocity data. The result of $\gamma^0>0$ indicates flood-dominance, and $\gamma^0<0$ indicates ebb-dominance, resulting in flood- and ebb-directed transport, respectively (Pritchard and Green, 2017).

The results of the near-surface and near-bottom tidal asymmetry are shown in Figure 5. Tidal asymmetry parameter was calculated for both cases over 31 days (02/11–03/13), including the spring–neap variations. The ebb-dominance of the NF for Case 2 were reduced compared to Case 1 in both the surface and bottom layers. Especially, near-bottom of the NF changed from ebb-dominance to flood-dominance. On the other hand, the ebb-dominance of the SF was enhanced in both the surface and bottom layers. These increase and decrease in tidal asymmetry also affect the residual flows (Wang, Jeuken, and De Vriend, 1999).

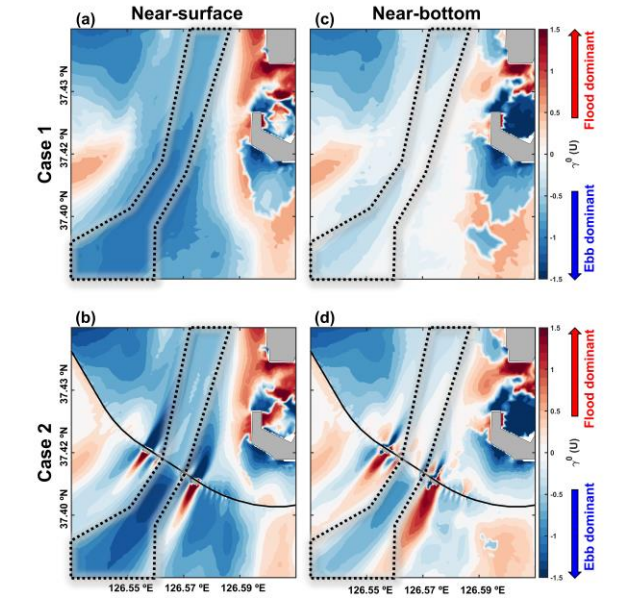

Figure 5. Spatial distribution of tidal asymmetry for near-surface and near-bottom in A1. The tidal asymmetry for Case 1 and Case 2: Near-surface (a and b), near-bottom (c and d). Black dashed line indicates the fairway and black solid line indicates IB.

The increased vertical salinity gradient near the bridge can enhance the tidal asymmetry (Teng *et al*., 2022). In Gyeonggi Bay, the horizontal gradient of water temperature is low at less than 5 degrees, whereas the gradient of salinity is high at more than 20 psu. Therefore, salinity differences eventually lead to density gradients, which can significantly affect residual flow patterns driven by the horizontal density gradients. This salinity gradient was reproduced in the model as distinctly changing at IB, which can be confirmed in the P1 and P2 residual flow dynamics.

Overall, the salinity gradient and tidal asymmetry were spatially modified due to the construction of the IB, which could cause changes in mass transport as the opposite residual patterns between the northern and southern ends of the IB were induced. This can lead to different results from Lee, Kim, and Woo (2023), and it is necessary to apply the piers of the bridge for modeling related to mass transport.

CONCLUSION

This research analyzed, the effect of the IB construction on the tidal- and residual flow patterns of the macrotidal environment, Gyeonggi Bay. After the construction of the IB, the salinity stratification near the piers of the bridge was strengthened, and the current velocity during flood and ebb was increased. On the north side of the navigation channel, the current magnitude increased mainly during flood, and on the south side increased during ebb. Due to these changes of salinity stratification and current magnitude, the tidal asymmetry of the navigation channel was modified. Effect of the decreased ebb-dominance on the northside of the fairway, the vertical two-layer flow structure of residual current was strengthened. In contrast, increased ebb-dominance on the southside of the fairway at all vertical water columns was unified into the ebb direction.

These results can occur morphological evolution of the fairway. Therefore, local structures such as IB can play an important role in more accurate model simulation to analyze estuarine circulation.

ACKNOWLEDGMENTS

This research was supported by Korea Institute of Marine Science & Technology Promotion (KIMST) funded by the Ministry of Oceans and Fisheries (20220051). This research was supported by a National Research Foundation of Korea Grant from the Korean Government (MSIT: the Ministry of Science and ICT) (NRF-2021M1A5A1075516) (KOPRI-PN22013).

LITERATURE CITED

Chen, C.; Beardsley, R.C.; Cowles, G.; Qi, J.; Lai, Z.; Gao, G.; Stuebe, D.; Xu, Q.; Xue, P.; Ge, J.; Ji, R.; Hu, S.; Tian, R.; Huang, H.; Wu, L., and Lin, H., 2013. *An Unstructured-Grid, Finite-Volume Community Ocean Model: FVCOM User Manual*. Cambridge, MA, USA: Sea Grant College Program, Massachusetts Institute of Technology, pp. 3-52

Kirby, R. and Retière, C., 2009. Comparing environmental effects of Rance and Severn barrages. *Proceedings of the Institution of Civil Engineers-Maritime Engineering*, 162(1), 11-26.

Lee, H.M.; Kim, J.W., and Woo, S.B., 2023. Mechanisms of advective and tidal oscillatory salt transport in the hypertidal estuary: Yeomha Channel in Gyeonggi Bay. *Journal of Marine Science and Engineering*, 11(2), 287.

Li, P.; Li, G.; Qiao, L.; Chen, X.; Shi, J.; Gao, F.; Wang, N., and Yue, S., 2014. Modeling the tidal dynamic changes induced by the bridge in Jiaozhou Bay, Qingdao, China. *Continental Shelf Research*, 84, 43-53.

Nidzieko, N.J. and Ralston, D.K., 2012. Tidal asymmetry and velocity skew over tidal flats and shallow channels within a macrotidal river delta. *Journal of Geophysical Research: Oceans*, 117(C3).

Park, K.; Oh, J.H.; Kim, H.S., and Im, H.H., 2002. Case study: Mass transport mechanism in Kyunggi Bay around Han River mouth, Korea. *Journal of Hydraulic Engineering*, 128(3), 257-267.

Pritchard, M. and Green, M., 2017. Trapping and episodic flushing of suspended sediment from a tidal river. *Continental Shelf Research*, 143, 286-294.

Teng, L.; Cheng, H.; Zhang, E., and Wang, Y., 2022. Lateral variation of tidal mixing asymmetry and its impact on the longitudinal sediment transport in turbidity maximum zone of salt wedge estuary. *Journal of Marine Science and Engineering*, 10(7), 907.

Wang, Z.B.; Jeuken, C., and De Vriend, H.J., 1999. Tidal asymmetry and residual sediment transport in estuaries. *Delft Hydraulics*, Z2749.

Willmott, C.J., 1982. Some comments on the evaluation of model performance. *Bulletin of the American Meteorological Society*, 63(11), 1309-1313.

Yamini, O.A.; Mousavi, S.H.; Kavianpour, M.R., and Safari Ghaleh, R., 2021. Hydrodynamic performance and cavitation analysis in bottom outlets of dam using CFD modelling. *Advances in Civil Engineering*, 2021, 1-14.

Yanagi, T.; Shimizu, M.; Nomura, M., and Furukawa, K., 2003. Spring–neap tidal variations of residual flow in Tokyo Bay, Japan. *Continental Shelf Research*, 23(11-13), 1087-1097.

Yeo, W.K.; Lee, H.; Kim, J.H., and Kwak, M.S., 2006. An interdisciplinary study on the scour depth estimation of Incheon Bridge. *Proceedings of the Korea Water Resources Association Conference*, 562-566.

Yeo, W.K.; Ji, W.; Kim, C.S., and Lim, J.C., 2008. Pier-scour characteristics of the marine bridge with ship impact protection - Incheon Bridge Case. *Journal of Korean Society of Coastal Ocean Engineers*, 20(2), 203-211.